

Analysis of Carbon Epoxy Shaft in Aerostatic Conical Journal Bearings — No Rotational Case

R B Ingle, *Non-member*

Dr B B Ahuja, *Member*

S M Joshi, *Associate Member*

In recent years demands for materials which exhibit high stiffness and high strength to weight ratio has increased. The use of advanced materials with high specific stiffness and high damping property for shafts may make it easier to realize high rotational speed with high stability. Composites of two materials one having a high Young's Modulus and the other high damping reflecting the best characteristics of each material, are likely candidates for such use. In this paper, one stepped carbon epoxy hollow shaft having 16 layers with total thickness 3.5 mm has been analysed for no rotational case. The mathematical analysis has been done for the conical aerostatic journal bearing in which the shaft rotates at high speed. The global and local stresses and strains at the top, middle and bottom of each layer corresponding to each of the stacking sequence for the shaft has been calculated.

Keywords : Composite shaft; Aerostatic conical journal bearing; Stacking sequence; Strength ratios; Failure envelope

NOTATION

E_x, E_y	: Young's modulus in x and y directions, respectively
h	: variable local film thickness ($h = \cos \alpha (1 + \varepsilon \cos \alpha (\theta_D / \sin \alpha))$), m
J	: rigidity or stiffness, N/m
L	: length of the conical bearing, m
M_x, M_y	: interaction parameters
P	: pressure, N/m ²
\bar{Q}	: reduced stiffness matrix corresponding to that of the ply located at the point
r	: variable radius of cone along the axis, m
r_L, r_s	: radii of the longer and smaller ends of the bearing, respectively, m
R, R_M	: variable and mean radii of the developed conical bearing sector, respectively, m
R_L, R_S	: larger and smaller end radii of the developed bearing sector, respectively, m
\bar{S}	: elements of compliance matrix for the laminate
α	: semi-cone angle of the bearing, degree
$\beta_x, \beta_y, \beta_{xy}$: moisture coefficients in x , y and x - y directions, respectively

Γ	: mass density, Ns ² /m ⁴
$\zeta_x, \zeta_y, \zeta_{xy}$: thermal expansion coefficients in x , y , and x - y directions, respectively
θ	: angular position from the point of maximum film thickness in the conical bearing, degree
θ_D	: subtended angle of the developed conical bearing sector, rad
μ	: absolute viscosity of air = 18.55×10^{-6} Ns/m ²
τ_{xy}	: shear modulus in x - y plane

INTRODUCTION

The employment of advanced materials with high specific stiffness and high damping property for the shaft may be more feasible to realize the high rotational speed with high stability. Moreover, it is very difficult to increase the dynamic stiffness of conventional materials because they usually have high stiffness with low damping and *vice versa*. Composite materials, on the other hand, can be composed of two materials, one of which has a high Young's Modulus and the other high damping. The resulting performance will reflect the best characteristics of each material.

The effect of circumferential flow using the continuity equation in externally pressurized air journal bearings has been reported by Majumdar¹. Cheng and Traupler² reported on the stability of the high speed journal bearing under steady load. Srinivasan and Prabhu³ have extensively analysed the externally pressurized gas lubricated conical bearing for its characteristics and the analysis confirms well to the present work. Ahuja⁴ has designed, developed a non-dimensional aerostatic and aerodynamic

R B Ingle and S M Joshi are with Mechanical Engineering Department, while Dr B B Ahuja is with Production Engineering Department, Pune Institute of Engineering and Technology, Pune 411 005.

This paper was received on October 22, 2002. Written discussion on the paper will be entertained till September 30, 2004.

Table 1 Material properties for carbon epoxy laminates

Longitudinal Young's Modulus	GPa	108.6
Transverse Young's Modulus	GPa	4.48
Major Poisson's Ratio		0.3533
In-plane Shear Modulus	GPa	1.6
Ply Thickness	Mm	0.21875
Longitudinal Tensile Strength	MPa	1.55E+03
Longitudinal Compressive Strength	MPa	4.7E+02
Transverse Tensile Strength	MPa	31.0
Transverse Compressive Strength	MPa	31.0
Inplane Shear Strength	MPa	31.0
Coefficient of Thermal Expansion Dir 1	µm/m/°C	-1.10E-06
Coefficient of Thermal Expansion Dir 2	µm/m/°C	1.0E-05
Coefficient of Moisture Expansion Dir 1	m/m/kg/kg	3.26E-02
Coefficient of Moisture Expansion Dir 2	m/m/kg/kg	7.4680-01

conical bearing for high speed machine tool applications. Stresses and deformations in cross ply composite tubes subjected to a uniform temperature change and stresses and deformations in thick walled cylinders subjected to combined loading and a temperature gradient have been dealt in detail by Tutunku^{5,6} and Hyer, *et al*⁷. The concise property relations for an anisotropic lamina are discussed by Reuter⁸. A general theory of strength for anisotropic materials has been presented by Tsai and Wu⁹.

In this paper, one stepped carbon epoxy shaft with total thickness 3.5 mm and 16 layers has been analysed. The mathematical analysis has been done for the conical aerostatic journal bearing in which the shaft rotates at high speed. The present study deals with the analysis for no rotational case of the shaft. For the said work the stacking sequence is [0/90/45/-45]_{2s}. Table 1 lists the material properties for the carbon epoxy laminate used in the present analysis.

MATHEMATICAL ANALYSIS FOR AEROSTATIC CONICAL JOURNAL BEARING—NO ROTATIONAL CASE

The general Reynolds equation for fluid for no rotational case in cylindrical co-ordinates for a conical bearing is

$$\frac{1}{r} \frac{\partial}{\partial r} \left(\frac{rh^3 \Gamma \partial P}{\mu \partial r} \right) + \frac{1}{r^2} \frac{\partial}{\partial \theta} \left(\frac{r^3 \Gamma \partial P}{\mu \partial \theta} \right) = 0 \quad (1)$$

where $\Gamma = \frac{P}{R_g T}$.

For an iso-thermal perfect gas film having constant viscosity, equation gets transformed to

$$\frac{\partial}{\partial r} \left(\frac{rh^3 \partial P^2}{\partial r} \right) + \frac{1}{r} \frac{\partial}{\partial \theta} \left(\frac{h^3 \partial P^2}{\partial \theta} \right) = 0 \quad (2)$$

or in developed form equation (2) is written as

$$\frac{1}{R \sin \alpha \sin \alpha} \frac{\partial}{\partial R} \left(\frac{R \sin \alpha h^3 \partial P^2}{2 \sin \alpha \partial R} \right) + \frac{1}{\sin^2 \alpha R^2} \frac{\partial}{\partial \theta} \left(\frac{h^3 \partial P^2}{2 \partial \theta} \right) = 0 \quad (3)$$

For a developed conical bearing

$$R \sin \alpha = R_s \sin \alpha + \frac{(J-8) \cos \alpha (R_L \sin \alpha - R_s \sin \alpha) R_M \Delta}{L} \quad (4)$$

where $\Delta = 24 \mu C_D A_O (k R_g T)^{1/2} / C_r^3 P_s$; C_D is orifice discharge coefficient; A_O , orifice cross-sectional area, m²; C_r , the concentric radial clearance 0.000 044 m; and P_s , the supply pressure, N/m².

Equation (4) is further expanded as

$$\frac{\partial Q}{\partial R} + \frac{\bar{R} \partial^2 Q}{\partial \bar{R}^2} + \frac{3}{R h} \frac{\partial \bar{h}}{\partial \theta} \frac{\partial Q}{\partial \theta} + \frac{1}{R} \frac{\partial^2 Q}{\partial \theta^2} = 0 \quad (5)$$

The mass flow rate from the larger and smaller ends of the bearing are calculated as

The circumferential mass flow M_{cm} is

$$M_{cm} = \int_0^{h_2} \int_{l_1}^{l_2} u \Gamma dz dy \quad (6)$$

where $u = \frac{1}{2\mu} \frac{\delta P}{\delta x} (z^2 - zh) + \frac{uz}{h}$.

u being the circumferential velocity; dy , the element under consideration along length; and dz , the element thickness along the radius.

$$M_{cm} = \int_0^{h_2} \int_{l_1}^{l_2} u \frac{P}{R_g T} dz dy \quad (7)$$

$$M_{cm} = \int_0^{h_2} \int_{l_1}^{l_2} \frac{P}{R_g T} \left[\frac{1}{2\mu} \frac{\delta P}{\delta x} (z^2 - zh) + \frac{uz}{h} \right] dz dy \quad (8)$$

$u=0$ for non-rotational case.

$$M_{cm} = \int_{l_1}^{l_2} \frac{P}{R_g T} \left[\frac{1}{2\mu} \frac{\delta P}{\delta x} \left(\frac{-h^3}{6} \right) \right] dy \quad (9)$$

$$M_{cm} = \int_{l_2}^{l_1} \frac{1}{24\mu R_g T} \frac{\delta P^2 h^3}{r \delta \theta} / \theta = \theta^1 dy \text{ (since } \delta x = r \delta \theta) \quad (10)$$

The equation (10) represents generalized circumferential flow for a conical bearing. In the present analysis, localised axial flow component of the circumferential flow at all the orifices is ignored and this well justified by the theoretical values obtained

and compared the experimental results. Work reported on conical bearings by Srinivasan and Prabhu³ takes into account the localised axial flow component of the circumferential flow, but has not been supported with experimental results.

The radial load equation can be written as

$$\int_0^{2\pi} \int_0^L (p - p_a) r d\theta \times d / \cos\theta \cos\alpha + w_r = 0 \quad (11)$$

Similarly for axial load

$$\int_0^{2\pi} \int_0^L (p - p_a) r d\theta \times d / \cos\theta \sin\alpha - w_a = 0 \quad (12)$$

MICROMECHANICAL AND MACROMECHANICAL ANALYSIS

Classical Lamination Theory

Classical lamination theory is useful in calculating stresses and strains in each lamina of a thin laminated structure.

The basic assumptions in this design are :

- (a) Fibers are uniformly distributed throughout the matrix.
- (b) Perfect bonding exists between fibres and matrix and matrix is free of voids.

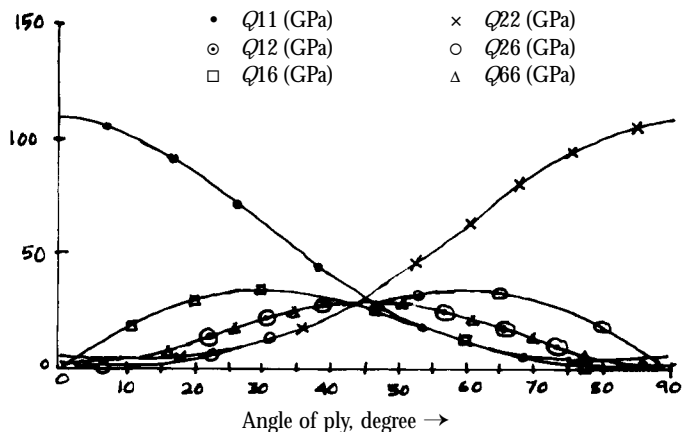


Figure 1 Variation of \bar{Q} with angle of ply

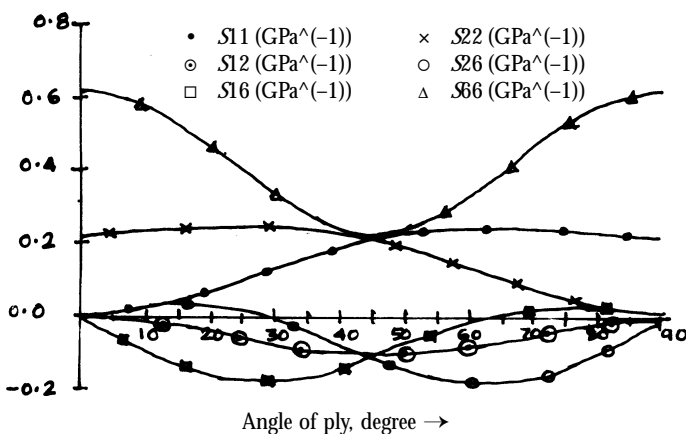


Figure 2 Variation of \bar{S} with angle of ply

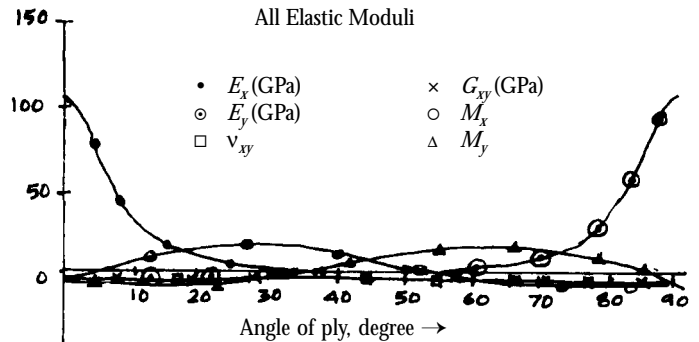


Figure 3 Variation of engineering constants with angle of ply

- (c) Applied loads are either parallel or normal to the fibre direction.
- (d) The lamina is in stress-free state initially.
- (e) Both fibres and matrix behave as linearly elastic materials.

Figures 1-3 depict variation of \bar{Q} , \bar{S} and engineering constants with angle of ply, respectively.

Failure Criteria

A composite laminate fails with increasing applied mechanical and thermal loads. The laminate failure may not be always catastrophic. It is possible that some layer(s) fail first and the composite continues to take more loads until all the plies fail. Failed plies may also contribute to the stiffness and strength properties of the laminate. The composite shaft may be subjected to axial, centrifugal and torsional loading. Stresses may be induced due to unbalance excitation, stresses in the radial direction and the interlaminar shear stresses may also play a dominant role in the various modes in which a shaft may fail.

Failure Envelopes

A failure envelope is a three-dimensional plot of the combinations of the normal and shear stresses which can be applied to an angle lamina just before failure. The failure envelopes are developed for constant shear stress and the two normal stresses are then used as the two axes. The basis for evaluation is that if the applied stress is within the failure envelope then the lamina is safe. Failure envelopes using the results obtained for all the four theories for a zero shear stress have been developed for the stacking sequence angles, namely, 0° , 45° , -45° and 90° (Figures 4-7). The values of stresses which can be applied are larger for 0° and 90° as compared to the values for 45° but then these are low in shear. As against this the values for 45° and -45° are in appreciable range and are strong in shear. These values are compared using different failure theories as mentioned in Appendix 1.

Figures 8 and 9 show variations of coefficients of thermal and moisture expansions, respectively with angle of ply. Figure 10 shows variation of theories with angle of ply.

All Theories : σ_y against σ_x

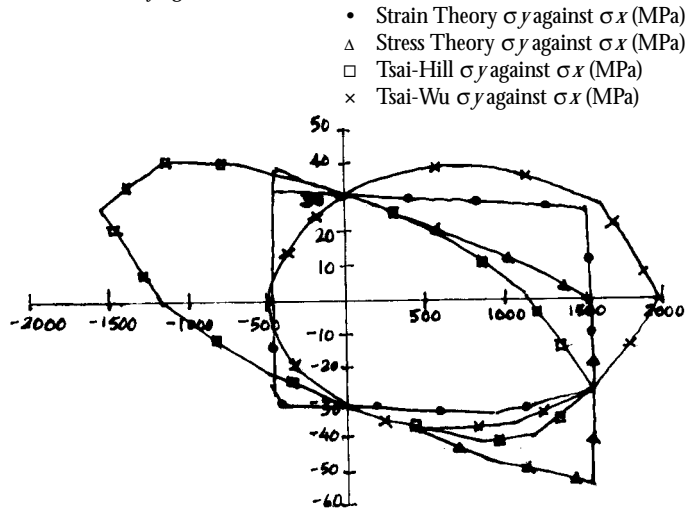


Figure 4 Failure envelope for angle of ply equal to zero

All Theories : σ_y against σ_x

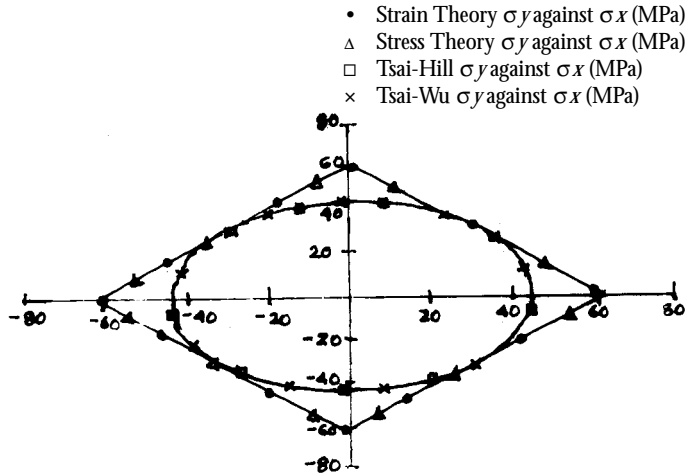


Figure 5 Failure envelope for angle of ply equal to 45°

All Theories : σ_y against σ_x

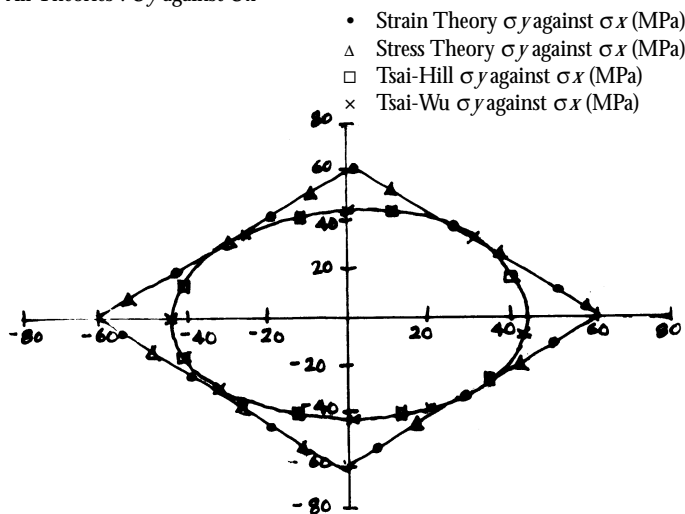


Figure 6 Failure envelope for angle of ply equal to -45°

All Theories : σ_y against σ_x (MPa)

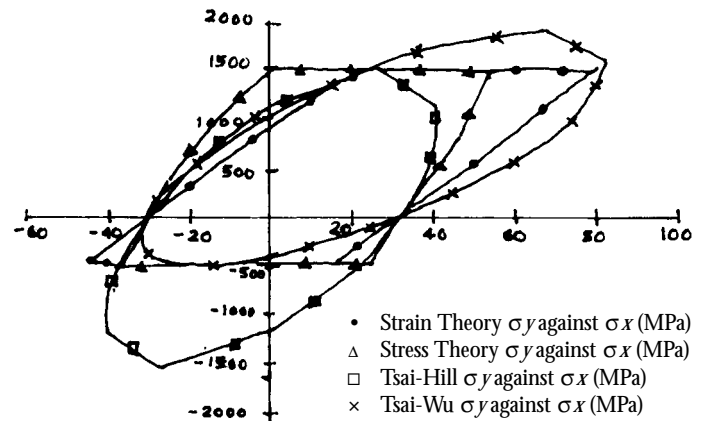


Figure 7 Failure envelope for angle of ply equal to 90°

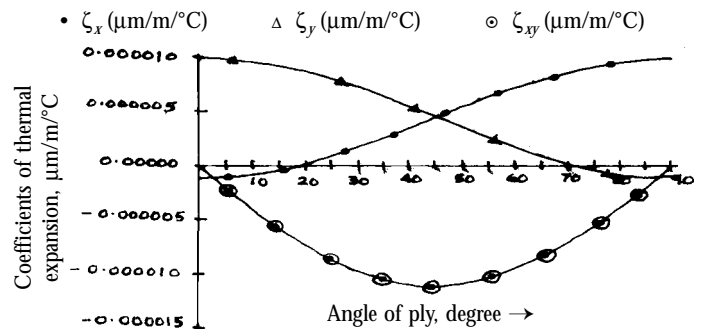


Figure 8 Variation of coefficients of thermal expansion with angle of ply

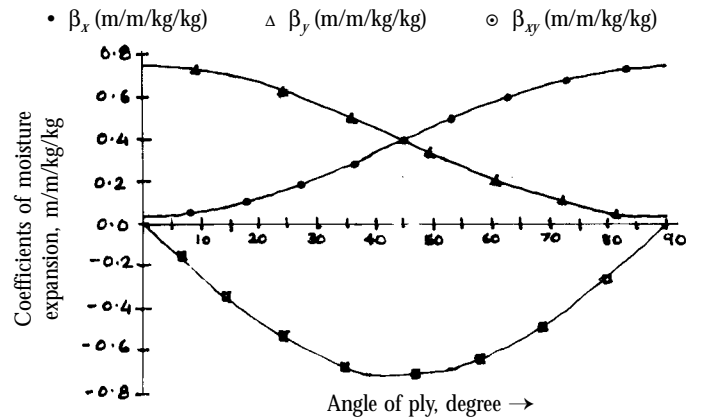


Figure 9 Variation of coefficients of moisture expansion with angle of ply

All Theories : Strength ratio-Carbon/Epoxy

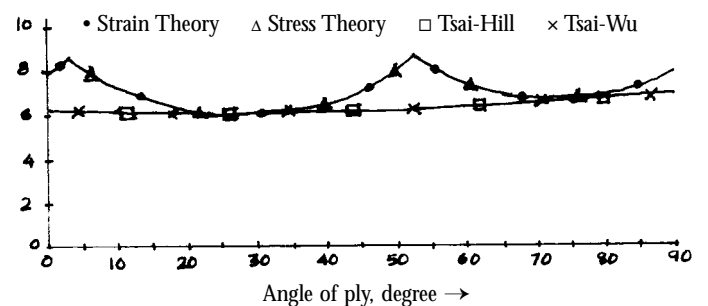


Figure 10 Variation of strain theory, stress theory, Tsai-Hill and Tsai-Wu theories with angle of ply

Table 2 Global stresses

			σ_1	σ_2	τ_{12}
Layer 1	Top		6.03E+06	-5.98E+06	1.77E-10
	0	Middle	6.03E+06	-5.98E+06	1.68E-10
		Bottom	6.03E+06	-5.98E+06	1.58E-10
Layer 2	Top		6.03E+06	-5.98E+06	-1.58E-10
	90	Middle	6.03E+06	-5.98E+06	-1.49E-10
		Bottom	6.03E+06	-5.98E+06	-1.41E-10
Layer 3	Top		6.03E+06	-5.98E+06	4.09E-09
	45	Middle	6.03E+06	-5.98E+06	4.09E-09
		Bottom	6.03E+06	-5.98E+06	4.09E-09
Layer 4	Top		6.03E+06	-5.98E+06	-4.09E-09
	-45	Middle	6.03E+06	-5.98E+06	-4.09E-09
		Bottom	6.03E+06	-5.98E+06	-4.09E-09
Layer 5	Top		6.03E+06	-5.98E+06	1.04E-10
	0	Middle	6.03E+06	-5.98E+06	9.50E-11
		Bottom	6.03E+06	-5.98E+06	8.59E-11
Layer 6	Top		6.03E+06	-5.98E+06	-8.59E-11
	90	Middle	6.03E+06	-5.98E+06	-7.68E-11
		Bottom	6.03E+06	-5.98E+06	-6.77E-11
Layer 7	Top		6.03E+06	-5.98E+06	4.09E-09
	45	Middle	6.03E+06	-5.98E+06	4.09E-09
		Bottom	6.03E+06	-5.98E+06	4.09E-09
Layer 8	Top		6.03E+06	-5.98E+06	-4.09E-09
	-45	Middle	6.03E+06	-5.98E+06	-4.09E-09
		Bottom	6.03E+06	-5.98E+06	-4.09E-09
Layer 9	Top		6.03E+06	-5.98E+06	-4.09E-09
	-45	Middle	6.03E+06	-5.98E+06	-4.09E-09
		Bottom	6.03E+06	-5.98E+06	-4.09E-09
Layer 10	Top		6.03E+06	-5.98E+06	4.09E-09
	45	Middle	6.03E+06	-5.98E+06	4.09E-09
		Bottom	6.03E+06	-5.98E+06	4.09E-09
Layer 11	Top		6.03E+06	-5.98E+06	5.12E-12
	90	Middle	6.03E+06	-5.98E+06	1.42E-11
		Bottom	6.03E+06	-5.98E+06	2.33E-11
Layer 12	Top		6.03E+06	-5.98E+06	-2.33E-11
	0	Middle	6.03E+06	-5.98E+06	-3.22E-11
		Bottom	6.03E+06	-5.98E+06	-4.15E-11
Layer 13	Top		6.03E+06	-5.98E+06	-3.66E-10
	-45	Middle	6.03E+06	-5.98E+06	-3.68E-10
		Bottom	6.03E+06	-5.98E+06	-3.66E-10
Layer 14	Top		6.03E+06	-5.98E+06	3.66E-10
	45	Middle	6.03E+06	-5.98E+06	3.66E-10
		Bottom	6.03E+06	-5.98E+06	3.66E-10
Layer 15	Top		6.03E+06	-5.98E+06	7.80E-11
	90	Middle	6.03E+06	-5.98E+06	8.71E-11
		Bottom	6.03E+06	-5.98E+06	9.62E-11
Layer 16	Top		6.03E+06	-5.98E+06	-9.62E-11
	0	Middle	6.03E+06	-5.98E+06	-1.05E-10
		Bottom	6.03E+06	-5.98E+06	-1.44E-10

Table 3 Local stresses

			σ_1	σ_2	τ_{12}
Layer 1	Top		6.03E+06	-5.98E+06	1.77E-10
	0	Middle	6.03E+06	-5.98E+06	1.68E-10
		Bottom	6.03E+06	-5.98E+06	1.58E-10
Layer 2	Top		6.03E+06	-5.98E+06	-1.58E-10
	90	Middle	6.03E+06	-5.98E+06	-1.49E-10
		Bottom	6.03E+06	-5.98E+06	-1.41E-10
Layer 3	Top		6.03E+06	-5.98E+06	4.09E-09
	45	Middle	6.03E+06	-5.98E+06	4.09E-09
		Bottom	6.03E+06	-5.98E+06	4.09E-09
Layer 4	Top		6.03E+06	-5.98E+06	-4.09E-09
	-45	Middle	6.03E+06	-5.98E+06	-4.09E-09
		Bottom	6.03E+06	-5.98E+06	-4.09E-09
Layer 5	Top		6.03E+06	-5.98E+06	1.04E-10
	0	Middle	6.03E+06	-5.98E+06	9.50E-11
		Bottom	6.03E+06	-5.98E+06	8.59E-11
Layer 6	Top		6.03E+06	-5.98E+06	-8.59E-11
	90	Middle	6.03E+06	-5.98E+06	-7.68E-11
		Bottom	6.03E+06	-5.98E+06	-6.77E-11
Layer 7	Top		6.03E+06	-5.98E+06	4.09E-09
	45	Middle	6.03E+06	-5.98E+06	4.09E-09
		Bottom	6.03E+06	-5.98E+06	4.09E-09
Layer 8	Top		6.03E+06	-5.98E+06	-4.09E-09
	-45	Middle	6.03E+06	-5.98E+06	-4.09E-09
		Bottom	6.03E+06	-5.98E+06	-4.09E-09
Layer 9	Top		6.03E+06	-5.98E+06	-4.09E-09
	-45	Middle	6.03E+06	-5.98E+06	-4.09E-09
		Bottom	6.03E+06	-5.98E+06	-4.09E-09
Layer 10	Top		6.03E+06	-5.98E+06	4.09E-09
	45	Middle	6.03E+06	-5.98E+06	4.09E-09
		Bottom	6.03E+06	-5.98E+06	4.09E-09
Layer 11	Top		6.03E+06	-5.98E+06	5.12E-12
	90	Middle	6.03E+06	-5.98E+06	1.42E-11
		Bottom	6.03E+06	-5.98E+06	2.33E-11
Layer 12	Top		6.03E+06	-5.98E+06	-2.33E-11
	0	Middle	6.03E+06	-5.98E+06	-3.22E-11
		Bottom	6.03E+06	-5.98E+06	-4.15E-11
Layer 13	Top		6.03E+06	-5.98E+06	-3.66E-10
	-45	Middle	6.03E+06	-5.98E+06	-3.68E-10
		Bottom	6.03E+06	-5.98E+06	-3.66E-10
Layer 14	Top		6.03E+06	-5.98E+06	3.66E-10
	45	Middle	6.03E+06	-5.98E+06	3.66E-10
		Bottom	6.03E+06	-5.98E+06	3.66E-10
Layer 15	Top		6.03E+06	-5.98E+06	7.80E-11
	90	Middle	6.03E+06	-5.98E+06	8.71E-11
		Bottom	6.03E+06	-5.98E+06	9.62E-11
Layer 16	Top		6.03E+06	-5.98E+06	-9.62E-11
	0	Middle	6.03E+06	-5.98E+06	-1.05E-10
		Bottom	6.03E+06	-5.98E+06	-1.44E-10

Table 4 Local strains

			ϵ_x	ϵ_y	γ_{xy}
Layer 1	Top		1.40E-04	1.40E-04	1.11E-19
	Middle	0	1.40E-04	1.40E-04	1.05E-19
	Bottom		1.40E-04	1.40E-04	9.92E-20
Layer 2	Top		1.40E-04	1.40E-04	-9.92E-20
	Middle	90	1.40E-04	1.40E-04	-9.35E-20
	Bottom		1.40E-04	1.40E-04	-8.78E-20
Layer 3	Top		1.40E-04	1.40E-04	-8.13E-20
	Middle	45	1.40E-04	1.40E-04	-8.13E-20
	Bottom		1.40E-04	1.40E-04	-8.13E-20
Layer 4	Top		1.40E-04	1.40E-04	8.12E-20
	Middle	-45	1.40E-04	1.40E-04	8.13E-20
	Bottom		1.40E-04	1.40E-04	8.12E-20
Layer 5	Top		1.40E-04	1.40E-04	6.51E-20
	Middle	0	1.40E-04	1.40E-04	5.94E-20
	Bottom		1.40E-04	1.40E-04	5.37E-20
Layer 6	Top		1.40E-04	1.40E-04	-5.37E-20
	Middle	90	1.40E-04	1.40E-04	-4.80E-20
	Bottom		1.40E-04	1.40E-04	-4.23E-20
Layer 7	Top		1.40E-04	1.40E-04	-1.08E-19
	Middle	45	1.40E-04	1.40E-04	-1.08E-19
	Bottom		1.40E-04	1.40E-04	-1.08E-19
Layer 8	Top		1.40E-04	1.40E-04	1.08E-19
	Middle	-45	1.40E-04	1.40E-04	1.08E-19
	Bottom		1.40E-04	1.40E-04	1.08E-19
Layer 9	Top		1.40E-04	1.40E-04	1.08E-19
	Middle	-45	1.40E-04	1.40E-04	1.08E-19
	Bottom		1.40E-04	1.40E-04	1.08E-19
Layer 10	Top		1.40E-04	1.40E-04	-1.08E-19
	Middle	45	1.40E-04	1.40E-04	-1.08E-19
	Bottom		1.40E-04	1.40E-04	-1.08E-19
Layer 11	Top		1.40E-04	1.40E-04	3.20E-21
	Middle	90	1.40E-04	1.40E-04	8.89E-21
	Bottom		1.40E-04	1.40E-04	1.46E-20
Layer 12	Top		1.40E-04	1.40E-04	-1.46E-20
	Middle	0	1.40E-04	1.40E-04	-2.03E-20
	Bottom		1.40E-04	1.40E-04	-2.60E-20
Layer 13	Top		1.40E-04	1.40E-04	1.35E-19
	Middle	-45	1.40E-04	1.40E-04	1.35E-19
	Bottom		1.40E-04	1.40E-04	1.35E-19
Layer 14	Top		1.40E-04	1.40E-04	-1.35E-20
	Middle	45	1.40E-04	1.40E-04	-1.35E-19
	Bottom		1.40E-04	1.40E-04	-1.35E-19
Layer 15	Top		1.40E-04	1.40E-04	4.87E-20
	Middle	90	1.40E-04	1.40E-04	5.44E-20
	Bottom		1.40E-04	1.40E-04	6.01E-20
Layer 16	Top		1.40E-04	1.40E-04	-6.01E-20
	Middle	0	1.40E-04	1.40E-04	-6.58E-20
	Bottom		1.40E-04	1.40E-04	-7.15E-20

Table 5 Global strains

			ϵ_x	ϵ_y	γ_{xy}
Layer 1	Top		1.40E-04	1.40E-04	1.11E-19
	Middle	0	1.40E-04	1.40E-04	1.05E-19
	Bottom		1.40E-04	1.40E-04	9.92E-20
Layer 2	Top		1.40E-04	1.40E-04	9.92E-20
	Middle	90	1.40E-04	1.40E-04	9.35E-20
	Bottom		1.40E-04	1.40E-04	8.78E-20
Layer 3	Top		1.40E-04	1.40E-04	8.78E-20
	Middle	45	1.40E-04	1.40E-04	8.25E-20
	Bottom		1.40E-04	1.40E-04	7.65E-20
Layer 4	Top		1.40E-04	1.40E-04	7.65E-20
	Middle	-45	1.40E-04	1.40E-04	7.08E-20
	Bottom		1.40E-04	1.40E-04	6.51E-20
Layer 5	Top		1.40E-04	1.40E-04	6.51E-20
	Middle	0	1.40E-04	1.40E-04	5.94E-20
	Bottom		1.40E-04	1.40E-04	5.37E-20
Layer 6	Top		1.40E-04	1.40E-04	5.37E-20
	Middle	90	1.40E-04	1.40E-04	4.80E-20
	Bottom		1.40E-04	1.40E-04	4.23E-20
Layer 7	Top		1.40E-04	1.40E-04	4.23E-20
	Middle	45	1.40E-04	1.40E-04	3.66E-20
	Bottom		1.40E-04	1.40E-04	3.09E-20
Layer 8	Top		1.40E-04	1.40E-04	3.09E-20
	Middle	-45	1.40E-04	1.40E-04	2.53E-20
	Bottom		1.40E-04	1.40E-04	1.96E-20
Layer 9	Top		1.40E-04	1.40E-04	1.96E-20
	Middle	-45	1.40E-04	1.40E-04	1.39E-20
	Bottom		1.40E-04	1.40E-04	8.18E-21
Layer 10	Top		1.40E-04	1.40E-04	8.18E-21
	Middle	45	1.40E-04	1.40E-04	2.49E-21
	Bottom		1.40E-04	1.40E-04	-3.20E-21
Layer 11	Top		1.40E-04	1.40E-04	-3.20E-21
	Middle	90	1.40E-04	1.40E-04	-8.89E-21
	Bottom		1.40E-04	1.40E-04	-1.46E-20
Layer 12	Top		1.40E-04	1.40E-04	-1.46E-20
	Middle	0	1.40E-04	1.40E-04	-2.03E-20
	Bottom		1.40E-04	1.40E-04	-2.60E-20
Layer 13	Top		1.40E-04	1.40E-04	-2.60E-20
	Middle	-45	1.40E-04	1.40E-04	-3.17E-20
	Bottom		1.40E-04	1.40E-04	-3.73E-20
Layer 14	Top		1.40E-04	1.40E-04	-3.73E-20
	Middle	45	1.40E-04	1.40E-04	-4.30E-20
	Bottom		1.40E-04	1.40E-04	-4.87E-20
Layer 15	Top		1.40E-04	1.40E-04	-4.87E-20
	Middle	90	1.40E-04	1.40E-04	-5.44E-20
	Bottom		1.40E-04	1.40E-04	-6.01E-20
Layer 16	Top		1.40E-04	1.40E-04	-6.01E-20
	Middle	0	1.40E-04	1.40E-04	-6.58E-20
	Bottom		1.40E-04	1.40E-04	-7.15E-20

Table 6 Strength ratios

			Max strain	Max stress	Tsai-Hill	Tsai-Wu
Layer 1	1	Top	1.692E4 (2T)	1.241E4 (2T)	1.16E+04	2.11E+04
	0	Middle	1.692E4 (2T)	1.241E4 (2T)	1.16E+04	2.11E+04
		Bottom	1.692E4 (2T)	1.241E4 (2T)	1.16E+04	2.11E+04
Layer 2	2	Top	1.692E4 (2T)	1.241E4 (2T)	1.16E+04	2.11E+04
	90	Middle	1.692E4 (2T)	1.241E4 (2T)	1.16E+04	2.11E+04
		Bottom	1.692E4 (2T)	1.241E4 (2T)	1.16E+04	2.11E+04
Layer 3	3	Top	1.692E4 (2T)	1.241E4 (2T)	1.16E+04	2.11E+04
	45	Middle	1.692E4 (2T)	1.241E4 (2T)	1.16E+04	2.11E+04
		Bottom	1.692E4 (2T)	1.241E4 (2T)	1.16E+04	2.11E+04
Layer 4	4	Top	1.692E4 (2T)	1.241E4 (2T)	1.16E+04	2.11E+04
	-45	Middle	1.692E4 (2T)	1.241E4 (2T)	1.16E+04	2.11E+04
		Bottom	1.692E4 (2T)	1.241E4 (2T)	1.16E+04	2.11E+04
Layer 5	5	Top	1.692E4 (2T)	1.241E4 (2T)	1.16E+04	2.11E+04
	0	Middle	1.692E4 (2T)	1.241E4 (2T)	1.16E+04	2.11E+04
		Bottom	1.692E4 (2T)	1.241E4 (2T)	1.16E+04	2.11E+04
Layer 6	6	Top	1.692E4 (2T)	1.241E4 (2T)	1.16E+04	2.11E+04
	90	Middle	1.692E4 (2T)	1.241E4 (2T)	1.16E+04	2.11E+04
		Bottom	1.692E4 (2T)	1.241E4 (2T)	1.16E+04	2.11E+04
Layer 7	7	Top	1.692E4 (2T)	1.241E4 (2T)	1.16E+04	2.11E+04
	45	Middle	1.692E4 (2T)	1.241E4 (2T)	1.16E+04	2.11E+04
		Bottom	1.692E4 (2T)	1.241E4 (2T)	1.16E+04	2.11E+04
Layer 8	8	Top	1.692E4 (2T)	1.241E4 (2T)	1.16E+04	2.11E+04
	-45	Middle	1.692E4 (2T)	1.241E4 (2T)	1.16E+04	2.11E+04
		Bottom	1.692E4 (2T)	1.241E4 (2T)	1.16E+04	2.11E+04
Layer 9	9	Top	1.692E4 (2T)	1.241E4 (2T)	1.16E+04	2.11E+04
	-45	Middle	1.692E4 (2T)	1.241E4 (2T)	1.16E+04	2.11E+04
		Bottom	1.692E4 (2T)	1.241E4 (2T)	1.16E+04	2.11E+04
Layer 10	10	Top	1.692E4 (2T)	1.241E4 (2T)	1.16E+04	2.11E+04
	45	Middle	1.692E4 (2T)	1.241E4 (2T)	1.16E+04	2.11E+04
		Bottom	1.692E4 (2T)	1.241E4 (2T)	1.16E+04	2.11E+04
Layer 11	11	Top	1.692E4 (2T)	1.241E4 (2T)	1.16E+04	2.11E+04
	90	Middle	1.692E4 (2T)	1.241E4 (2T)	1.16E+04	2.11E+04
		Bottom	1.692E4 (2T)	1.241E4 (2T)	1.16E+04	2.11E+04
Layer 12	12	Top	1.692E4 (2T)	1.241E4 (2T)	1.16E+04	2.11E+04
	0	Middle	1.692E4 (2T)	1.241E4 (2T)	1.16E+04	2.11E+04
		Bottom	1.692E4 (2T)	1.241E4 (2T)	1.16E+04	2.11E+04
Layer 13	13	Top	1.692E4 (2T)	1.241E4 (2T)	1.16E+04	2.11E+04
	-45	Middle	1.692E4 (2T)	1.241E4 (2T)	1.16E+04	2.11E+04
		Bottom	1.692E4 (2T)	1.241E4 (2T)	1.16E+04	2.11E+04
Layer 14	14	Top	1.692E4 (2T)	1.241E4 (2T)	1.16E+04	2.11E+04
	45	Middle	1.692E4 (2T)	1.241E4 (2T)	1.16E+04	2.11E+04
		Bottom	1.692E4 (2T)	1.241E4 (2T)	1.16E+04	2.11E+04
Layer 15	15	Top	1.692E4 (2T)	1.241E4 (2T)	1.16E+04	2.11E+04
	90	Middle	1.692E4 (2T)	1.241E4 (2T)	1.16E+04	2.11E+04
		Bottom	1.692E4 (2T)	1.241E4 (2T)	1.16E+04	2.11E+04
Layer 16	16	Top	1.692E4 (2T)	1.241E4 (2T)	1.16E+04	2.11E+04
	0	Middle	1.692E4 (2T)	1.241E4 (2T)	1.16E+04	2.11E+04
		Bottom	1.692E4 (2T)	1.241E4 (2T)	1.16E+04	2.11E+04

RESULTS AND DISCUSSIONS

Figure 1 shows the variation of values of \bar{Q} with respect to the angle of ply. It is observed that Q_{11} decreases with increase in angle of ply. It is maximum at 0° . Similarly, Q_{22} increases with increase in the angle of ply. All the \bar{Q} intersect at 45° . This characteristic may be attributed to the stress invariants on which the values of the Q matrix are dependant. The value of S_{66} as seen from Figure 2 decreases till 45° and then increases till 90° . The value of S_{11} increases while the value of S_{22} decreases with increasing angle of ply. The values of \bar{S} intersect at 45° . The values of S_{12} , S_{16} and S_{26} follow a negative trend with increasing angle of ply. S_{16} moves towards the positive side while S_{26} moves towards the negative side with increasing angle of ply. E_x decreases with increase in ply angle. It is maximum at 0° . E_y follows the reverse trend and it is maximum at 90° . The in-plane shear modulus increases till 45° and then decrease as the angle of ply is further increased (Figure 3). From Figures 8 and 9 it is observed that the coefficient of thermal expansion and the coefficient of moisture expansion in the x -direction increases with increase in the angle of ply. A reverse trend is observed in the y -direction. The values of these coefficients first decrease till the value of 45 is reached and then goes on increasing beyond 45° in the x - y plane. Tables 2 and 3 exhibit the global and the local stresses, respectively and the local strains and the global strains are as in Tables 4 and 5, respectively. The values in the tables show the stress and the strain distribution at the top, middle and bottom of each layer for the applied loads. The trend followed in the distribution of the stresses σ_1 and σ_2 is same for all the layers whereas the shear stress τ_{12} is maximum in the middle portion of the laminate. The strains also follow the same distribution pattern as followed by the stresses. Strength ratio is the ratio of the maximum load which can be applied to the load actually applied. The concept of strength ratio is applicable to any of the failure theories as mentioned in Appendix 1. The concept is that if $SR > 1$ then the lamina is safe and the applied stress can be increased by a factor equal to the strength ratio. If $SR < 1$ then the lamina is unsafe and the value of the stress needs to be reduced by a factor equal to SR . A value of $SR = 1$ implies the failure load. Figure 10 shows the values of the strength ratios for the different theories as against the angle of ply. Table 6 gives the strength ratios for each ply at the top, middle and bottom of each layer corresponding to the applied mechanical and the hygrothermal loads.

REFERENCES

1. B C Majumdar. 'Theoretical Analysis of Externally Pressurised Bearings'. *Journal of Mechanical Engineering Science*, vol 12, no 2, 1970, p 123-129.

2. H S Cheng and P R Traupler. 'Stability of the High Speed Journal Bearing under Steady Load'. *Journal of Engineering for Industry. Trans ASME, Series B*, vol 85, 1963, p 274.
3. K Srinivasan and B S Prabhu. 'Analysis of Externally Pressurized Gas Lubricated Conical Bearings'. *Wear Journal*, vol 86, 1983, p 202-210.
4. B B Ahuja. 'Computer Aided Study and Analysis of Dynamic Characteristics of a CNC Machining System'. *PhD Thesis*, 1996.
5. N Tutunku. 'Radial Stresses in Composite Thick Walled Shafts'. *Journal of Applied Mechanics*, vol 62, 1995, p 547-549.
6. N Tutunku and S J Winckler. 'Stresses and Deformations in Thick Walled Cylinders Subjected to Combined Loading and a Temperature Gradient.' *J Reinforced Plastics and Composites*, vol 12, no 2, p 198-209.
7. M W Hyer, E Cooperd and D Cohen. 'Stresses and Deformations in Cross Ply Composite Tubes Subjected to a Uniform Temperature Change.' *J Thermal Stresses*, vol 9, 1986, p 97-117.
8. R C Reuter (Jr). 'Concise Property Relations for an Anisotropic Lamina'. *Journal of Composite Mater*, vol 6, 1971, p 270-274.
9. S W Tsai and E M Wu. 'A General Theory of Strength for Anisotropic Materials.' *Journal of Composite Mater*, vol 5, 1971, p 58-61.
10. S W Tsai and H T Hahn. 'Introduction to Composite Materials'. *Technomic*, Lancaster, Pa, 1980.

APPENDIX

Strain and Stress in a Laminate

If the strains are known at any point along the thickness of the laminate then the global stresses in each lamina can be calculated as

$$\begin{bmatrix} \sigma_{xx} \\ \sigma_{yy} \\ \tau_{xy} \end{bmatrix} = \begin{bmatrix} \bar{Q}_{11} & \bar{Q}_{12} & \bar{Q}_{16} \\ \bar{Q}_{21} & \bar{Q}_{22} & \bar{Q}_{26} \\ \bar{Q}_{16} & \bar{Q}_{26} & \bar{Q}_{66} \end{bmatrix} = \begin{bmatrix} \varepsilon_{xx} \\ \varepsilon_{yy} \\ \gamma_{xy} \end{bmatrix} = [\bar{Q}] \begin{bmatrix} \varepsilon_{xx} \\ \varepsilon_{yy} \\ \gamma_{xy} \end{bmatrix}$$

Failure Theories

Maximum Stress Theory

The Maximum Stress Theory states that the lamina is considered failed if

$$\begin{aligned} &-(\sigma_1^C)_{ult} < \sigma_1 < (\sigma_1^T)_{ult} \\ &-(\sigma_2^C)_{ult} < \sigma_2 < (\sigma_2^T)_{ult} \\ &-(\tau_{12})_{ult} < \tau_{12} < (\tau_{12})_{ult} \\ &(\sigma_1^T)_{ult} = \text{Ultimate longitudinal tensile strength (in direction 1)} \\ &(\sigma_1^C)_{ult} = \text{Ultimate longitudinal compressive strength (in direction 1)} \\ &(\sigma_2^T)_{ult} = \text{Ultimate transverse strength (in direction 2)} \\ &(\sigma_2^C)_{ult} = \text{Ultimate transverse compressive strength (in direction 2)} \\ &(\tau_{12})_{ult} = \text{Ultimate in-plane shear strength (in plane 1-2)} \end{aligned}$$

Maximum Strain Theory

$$\begin{aligned} &-(\varepsilon_1^C)_{ult} < \varepsilon_1 < (\varepsilon_1^T)_{ult} \\ &-(\varepsilon_2^C)_{ult} < \varepsilon_2 < (\varepsilon_2^T)_{ult} \\ &-(\gamma_{12})_{ult} < \gamma_{12} < (\gamma_{12})_{ult} \\ &(\varepsilon_1^T)_{ult} = \text{Ultimate longitudinal tensile strain (in direction 1)} \end{aligned}$$

- $-(\epsilon_1^C)_{ult}$ =Ultimate longitudinal compressive strain (in direction 1)
- $(\epsilon_2^T)_{ult}$ =Ultimate transverse tensile strain (in direction 2)
- $-(\epsilon_2^C)_{ult}$ =Ultimate transverse compressive strain (in direction 2)
- $(\gamma_{12})_{ult}$ =Ultimate in-plane shear strain (in plane 1-2)

Tsai-Hill Theory

$$[\sigma_1/(\sigma_1^T)_{ult}]^2 - [\sigma_1\sigma_1/(\sigma_1^T)_{ult}^2] + [\sigma_2/(\sigma_2^T)_{ult}]^2 + [\tau_{12}/(\tau_{12})_{ult}]^2 < 1$$

Tsai-Wu Theory

$$H_1\sigma_1 + H_2\sigma_2 + H_6\tau_{12} + H_{11}\sigma_1^2 + H_{22}\sigma_2^2 + H_{66}\tau_{12}^2 + 2H_{12}\sigma_1\sigma_2 < 1$$

The components $H_1, H_2, H_6, H_{11}, H_{22}, H_{66}$ and H_{12} of the failure theory are found using the strength parameters of the unidirectional lamina as

$$\begin{aligned} H_1(\sigma_1^T)_{ult} + H_{11}(\sigma_1^T)_{ult}^2 &= 1 \\ H_1(\sigma_1^C)_{ult} + H_{11}(\sigma_1^C)_{ult}^2 &= 1 \\ H_2(\sigma_2^T)_{ult} + H_{22}(\sigma_2^T)_{ult}^2 &= 1 \\ -H_2(\sigma_2^C)_{ult} + H_{22}(\sigma_2^C)_{ult}^2 &= 1 \\ H_6(\tau_{12})_{ult} + H_{66}((\tau_{12})_{ult})_{ult}^2 &= 1 \\ -H_6(\tau_{12})_{ult} + H_{66}((\tau_{12})_{ult})_{ult}^2 &= 1 \end{aligned}$$

and as per Tsai-Hill failure theory the empirical relation for $H_{12} = -1/2(\sigma_1^T)_{ult}^2$.